KHAN, M.A., JAFFERY, S.H.I., KHAN, M., YOUNAS, M., BUTT, S.I., AHMAD, R. and WARSI, S.S. 2020. Multi-objective optimization of turning titanium-based alloy Ti-6Al-4V under dry, wet, and cryogenic conditions using gray relational analysis (GRA). *International journal of advanced manufacturing technology* [online], 106(9-10), pages 3897-3911. Available from: https://doi.org/10.1007/s00170-019-04913-6

Multi-objective optimization of turning titanium-based alloy Ti-6Al-4V under dry, wet, and cryogenic conditions using gray relational analysis (GRA).

KHAN, M.A., JAFFERY, S.H.I., KHAN, M., YOUNAS, M., BUTT, S.I., AHMAD, R. and WARSI, S.S.

2020

This version of the article has been accepted for publication, after peer review (when applicable) and is subject to Springer Nature's AM terms of use, but is not the Version of Record and does not reflect post-acceptance improvements, or any corrections. The Version of Record is available online at: https://doi.org/10.1007/s00170-019-04913-6

OpenAIR @RGU

This document was downloaded from https://openair.rgu.ac.uk

SEE TERMS OF USE IN BOX ABOVE

DISTRIBUTED UNDER LICENCE

Multi-objective optimization of turning titanium-based alloy Ti-6Al-4V under dry, wet, and cryogenic conditions using gray relational analysis (GRA)

Muhammad Ali Khan [1], Syed Husain Imran Jaffery [1], Mushtaq Khan [1], Muhammad Younas [1], Shahid Ikramullah Butt [1], Riaz Ahmad [1], Salman Sagheer Warsi [2]

1. School of Mechanical and Manufacturing Engineering, National University of Sciences and Technology (NUST), Sector H-12, Islamabad 44000, Pakistan

2. Capital University of Science and Technology (CUST), Islamabad, Pakistan

Corresponding author: Syed Husain Imran Jaffery - imran@smme.nust.edu.pk

Abstract

In modern manufacturing industries, the importance of multi-objective optimization cannot be overemphasized particularly when the desired responses are differing in nature towards each other. With the emergence of new technologies, the need to achieve overall efficiency in terms of energy, output, and tooling is on the rise. Resultantly, endeavor is to make the machining process sustainable, productive, and efficient simultaneously. In this research, the effects of machining parameters (feed, cutting speed, depth of cut, and cutting condition including dry, wet, and cryogenic) were analyzed. Since sustainable production demands a balance between production quality and energy consumption, therefore, response parameters including specific cutting energy, tool wear, surface roughness, and material removal rate were considered. Taguchi-gray integrated approach was adopted in this study. Multi-objective function was developed using gray relational methodology, and its regression analysis was conducted. Response surface optimization was carried out to optimize the formulated multi-objective function and derive the optimum machining parameters. Concurrent responses were optimized with best-suited values of input parameters to make the most out of the machining process. Analysis of variance results showed that feed is the most effective parameter followed by cutting condition in terms of overall contribution in multi-objective function. The proposed optimum parameters resulted in improvement of tool wear and surface roughness by 30% and 22%, respectively, whereas specific cutting energy was reduced by 4%.

Keywords:- Titanium; Ti-6Al-4 V; Cryogenic machining; Sustainable machining; Multi-objective optimization; Gray relational grade; Response surface methodology

Nomenclature

AHP	Analytic hierarchy process
MRR	Material removal rate (cm^3/s)
ANOVA	Analysis of Variance
R	Wear rate
D	Workpiece diameter (mm)
Ra	Surface roughness (μm)
d	Depth of cut (mm)
RSM	Response surface methodology
f	Feed (mm/rev)
SCE	Specific cutting energy
GRA	Gray relational analysis
t	Cutting time
GRC	Gray relational coefficient
TOPSIS	Technique for order of preference by similarity to ideal solution
GRG	Gray relational grade
V	Cutting speed (m/min)
l_s	Spiral length of cut (mm)
VB	Flank wear (mm)
MOO	Multi-objective optimization

1 Introduction

Past few decades has seen exponential growth in industries in terms of technology, output, and efficiency. The focus is on increasing output quantity while ensuring sustainability and improving quality. This desire of excellence has fueled the need of optimization in machine and process domains. Energy, quality, and productivity are the three main avenues for research in today's manufacturing scenario [1]. These parameters are defined by different output responses which are optimized collectively to improve the manufacturing systems. About 20% of energy consumed worldwide is used in the manufacturing industry [2]. In addition to the obvious economic impact, this huge consumption has a significant 90% environmental impact [3]. According to one report, the manufacturing sector accounts for almost 13% of total CO_2 emissions worldwide [4]. Hence the optimization of energy parameters is of utmost importance. Machining accounts for almost 10% of all manufacturing usage [5]. Turning is an efficient and economical machining process having benefits of intricate part machiability with less complicated setup and greater production [6].

Titanium alloy Ti-6Al-4 V by virtue of its excellent physical and mechanical properties as shown in Table 1 accounts for almost 60% of all titanium alloy usage [8]. On the other hand, limiting factors on utilization of Ti-6Al-4 V includes low elastic modulus, high temperature strength, and poor thermal conduction [9]. Low thermal conductivity acts as a catalyst in chemical reactivity of titanium with the tool owing to attainment of higher temperatures during cutting operations [10]. Keeping in view the significant tool wear during machining of hard to cut materials, past researchers have used various cooling techniques like traditional high pressure coolant (HPC) [11, 12], minimum quantity lubrication (MQL)[13–15], and then lately cryogenic coolants [16–22]. Since about 20% of the total manufacturing cost can be attributed to coolants [23, 24], its influence on overall efficiency has to be gauged for overall optimization. Multi-objective optimization (MOO) can produce an optimized solution to complex input domain. Such technique seeks trade-off among machining parameters which otherwise influences the responses in a varying manner. Different researchers have used different techniques to achieve MOO. Bhushan [25] carried out the optimization technique using response surface methodology (RSM) taking speed, cutting depth, feed, and radius of tool nose into account during turning of 7075 Al alloy. Tool wear and power consumption were reduced by 22% and 14%, respectively, using optimum machining conditions. Using the same technique, Camposeco-Negrete [26] found feed as the most influential element affecting surface roughness whereas energy consumption was mainly influenced by cutting depth along with feed. Kumar et al. [27] simultaneously optimized surface integrity, productivity, and power consumption using Taguchi design of experiment. Technique for order preference by similarity to ideal solution (TOPSIS) method was adopted to obtain multi-performance composite index (MPCI). It was found that for MPCI with analytic hierarchy process (AHP) weights, depth of cut was the vital factor whereas for MPCI with equal and entropy weights nose radius became the significant input. Warsi et al. [28] conducted MOO during turning of Al 6061 T6 alloy. After assessing independent effects, RSM was employed for optimization. It was concluded that feed is the most influential parameter. Specific cutting energy and material removal rate were improved by 5% and 33%, respectively, using optimum machining parameters.

Desirability function approach was used by Gupta et al.[29] to investigate responses including tool life, surface integrity, and cutting forces during turning of grade 2 titanium alloy under MQL conditions. Investigation showed that overall optimization was attained at 200 m/min cutting speed, 0.10 mm/rev feed, and 90o cutting edge angle. Mia et al. [30] optimized turning of Ti-6Al-4 V using gray relational analysis. Cutting condition (dry and HPC) was selected as input variable along with feed and speed. Multi-objective analysis concluded that overall optimization was achieved at 165 m/min

Table 1 Properties of aerospace alloys at room temperature (adapted from [7])

Property	Material					
	Titanium	Ti-6Al-4 V	Ti-6Al-6 V-2Sn	Ti-10 V-2Fe-3Al	Inconel 718	Al 7075-T6 Alloy
Density (g/cm^3)	4.5	4.43	4.54	4.65	8.22	2.81
Hardness (HRC)	10–12 (equivalent)	30–36	38	32	38–44	~7 (equivalent)
Ultimate tensile strength (MPa)	220	950	1050	970	1350	572
Yield strength (MPa)	140	880	980	900	1170	503
Modulus of elasticity (GPa)	116	113.8	110	110	200	71.7
Ductility (%)	54	14	14	9	16	11
Fracture toughness (MPa m$^{1/2}$)	70	75	60	–	96.4	20–29
Thermal conductivity (W/mK)	17	6.7	6.6	7.8	11.4	130
Max. operating temperature (°C)	~150	315	315	315	650	–

cutting speed and 0.12 mm/rev feed under HPC conditions. Ramana et al.[31] carried out MOO taking basic input cutting parameters while turning Ti-6Al-4 V. Feed resulted as the most significant parameter. Effect of coating material under different cutting conditions (dry, wet, and cryogenic) on drillability of Inconel 718 was investigated by Ucak and Cicek [32]. It was found that although cryogenic drilling improved surface integrity and hole quality, the tool life was negatively affected due to excessive chipping and enhanced thrust force. Taguchi-gray augmented approach was used for collective optimization of surface integrity and tool life during turning of cobalt alloy Haynes 25 [33]. Vegetable-based cutting fluid with flow rate of 180 mL/h and cutting speed of 30 m/min gave optimized output. Overall cutting fluid was found to be the most significant variable. A comparative optimization study [34] was carried out taking different cooling conditions including high-pressure jet, cryogenic, MQL and MQL with nanofluid during machining of super alloy Inconel 718. Other input variables included feed, speed, and rake angle. It was concluded that cryogenic environment produced most favorable results in terms of tool wear. Mia et al. [35] conducted multi-objective optimization through Taguchi-gray integrated approach taking various responses including cutting force, specific energy, temperature, surface roughness, and material removal rate using single and dual cryogenic jet configuration. Desired targets were achieved at lower feed and higher speed values. A recent study performed MOO of Ti-6Al-4 V under dry conditions [36]. Tool wear and surface roughness were improved by 7% and 2% under optimum conditions whereas specific cutting energy was reduced by 6%. Present research has taken the previous work a step further by incorporating the machining environment including dry, wet, and cryogenic as input variable.

2 Research motivation

Specific cutting energy (SCE) and tool wear rate (R) are vital signs for sustainability of any machining system whereas productivity index includes material removal rate (MRR) and surface roughness (Ra). This research is based on the fact that these key output parameters need to be optimized collectively to maximize the sustainability, productivity, and efficiency of machining processes. Cutting conditions (dry, wet, cryogenic) are vested as input variable to fully benefit from the optimized values of other machining parameters. Taguchi-gray integrated approach is adopted to highlight the importance of MOO as individual responses are dissimilar in nature. This approach has been previously applied with different materials [28, 33] or with different set of parameters [30, 31, 35, 36]. The aim is to formulate and optimize a multi-objective function in terms of input parameters which is sustainable, productive, and efficient at the same time.

3 Experimental details

A comprehensive experimental layout was developed keeping in view the various machining environment requirements including dry, wet, and cryogenic conditions. Various aspects of experimental methodology are discussed below:

3.1 Experimental setup

Turning was performed on Ti-6Al-4 V bar using computerized numerical control (CNC) turning center ML-300. Machining setup is shown in Fig. 1. Rated power and maximum spindle speed were 26 kW and 3500 RPM, respectively. Chemical composition of workpiece as found in optical emission spectroscopy is given in Table 2 which is in conformance with ASTM B265–15 for Ti-6Al-4 V [37]. Uncoated Sandvik cutting inserts (CCMW 09 T3 04 H13) were used with 0^{o} rake angle and without chip breaker. Carbide tool was selected for experiments owing to its impact strength and toughness in cryogenic conditions [38]. A new insert was used in every experimental run for later inspection and record.

3.2 Machining environments

Three types of cutting conditions were used in the present research, namely; dry, wet, and cryogenic. Dry runs were conducted in absence of any cooling media. For wet runs, CNC Turning center ML-300 uses bio-stable water-soluble Shell Dromus B cutting oil at flow rate of 6 lit/min. Cryogenic cooling system was arranged as shown in Fig. 2. High pressure cylinder XL-160 (160 l capacity) was used to store liquid nitrogen (LN2). LN2 is most widely used among all cryogenics because of its inert nature and global availability [39]. Furthermore, literature highlights the enhanced effectiveness of LN2 when used between uncoated carbide tool and Ti alloy workpiece [40]. Pressure regulator kept a steady pressure of 20 psi. Vacuum-insulated cryogenic pipes were used to carry the media to a bifurcated cryogenic needle valve. Previous researches [35, 41, 42] have found that dual jets are the most efficient configuration for extending tool life. Therefore, two copper pipes (dia 4 mm) were used to impinge the cryogenic media, one each at flank and rake face with collective flow rate of 4 lit/min.

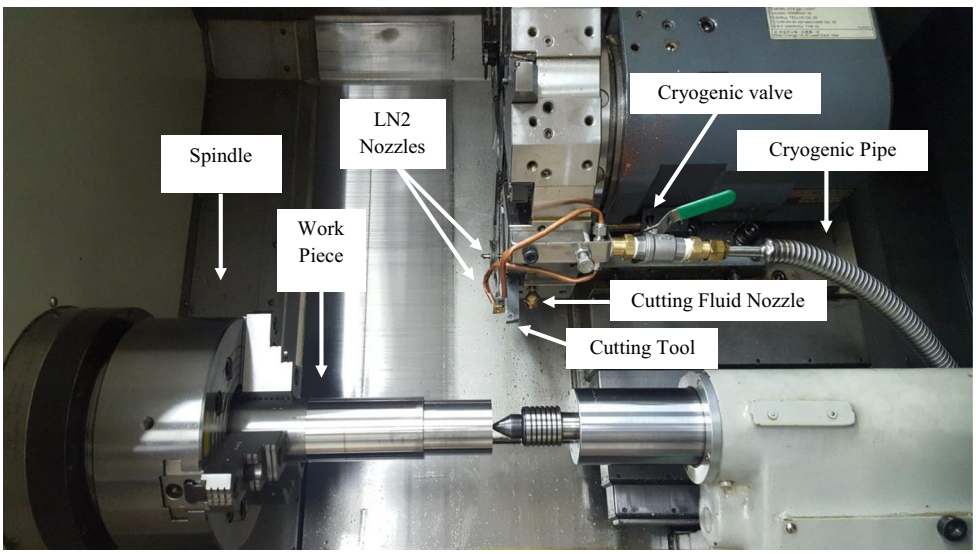

Fig. 1 Experimental machining setup

3.3 Selection of machining parameters

Cutting speed (v), feed (f), depth of cut (d), and cutting con-ditions (CC) (dry, wet, cryogenic) have significant effects on SCE, R, Ra, and MRR [27, 28, 34, 35]. Hence v, f, d, and CC were taken as the four input parameters. The selected levels and range of these input parameters were based on literature [36, 43], concerned ISO standards [44] and tool manufacturer guidelines (cutting speed 45–180 m/min, feed 0.01–0.26 mm/rev, depth of cut 0.01–4.5 mm) [45]. Table 3 presents the selected cutting parameters with their designated levels.

3.4 Measured responses

SCE, R, Ra, and MRR were measured as output responses. ISO 3685 criterion of average flank wear of 0.3 mm or maximum flank wear of 0.6 mm was followed for tool wear. Optical microscope was used for wear measurement. Figure 3 shows the flank wear measurement of a worn-out tool.

Tool wear rate was calculated using Eq. 1. A lower tool wear is indicated by a higher negative value of R.

$$R = \log\left[\frac{VB}{l_s}\right] = \left[\frac{VB}{1000tV}\right] \tag{1}$$

Here, V represents cutting velocity (m/min). Eq. (2) is used to work out the machining time.

$$t = \left[\frac{\pi D l_s}{1000fV}\right] \tag{2}$$

Table 2 Workpiece chemical composition (wt.%)

Ti	V	Al	Fe	Cu	Cr
89.44	4.2	5.7	0.15	0.003	0.0023

Ra was calculated using piezoelectric roughness tester times TR 110 with measuring range 0.05–10.0 μm. Multiple readings were taken at different points to eliminate variations. Power consumed during machining was calculated by Yokogawa power analyzer CW-240-F clamp-on meter (measurement interval 0.1 s). Two-cycle approach previously utilized effectively by different researchers [28, 36, 42, 46] was used. SCE is the amount of energy required to remove unit volume of material. It was determined using Eq. 3. It is highlighted that SCE is independent of make, type, and power rating of machine tool and its mechanical or electrical efficiency [36, 43, 47]. The machine tool independence was accomplished by carrying out selected runs on various machine tools.

$$\mathrm{SCE}\left(\mathrm{J/mm^3}\right) = \frac{\mathrm{P_{cut}(W)}}{\mathrm{MRR(mm^3/s)}} \tag{3}$$

In the above Eq., P_{cut} is the actual cutting power expanded on productive work. It is calculated by taking the difference (Eq. 4) of P_{acutal} and P_{air}. Here, P_{air} is the power required by machine for energizing its components including motor and pumps, short of actual cutting whereas P_{actual} corresponds to the power consumed during actual cutting in which the tool workpiece contact takes place.

$$\mathrm{P_{cut}(W)} = \mathrm{P_{actual}(W)} - \mathrm{P_{air}(W)} \tag{4}$$

P_{cut} is the machining power which when divided with MRR, i.e., amount of material removed per unit time gives the specific cutting energy in Joules per mm^3. MRR is the product of f, V, and d as shown in Eq. 5.

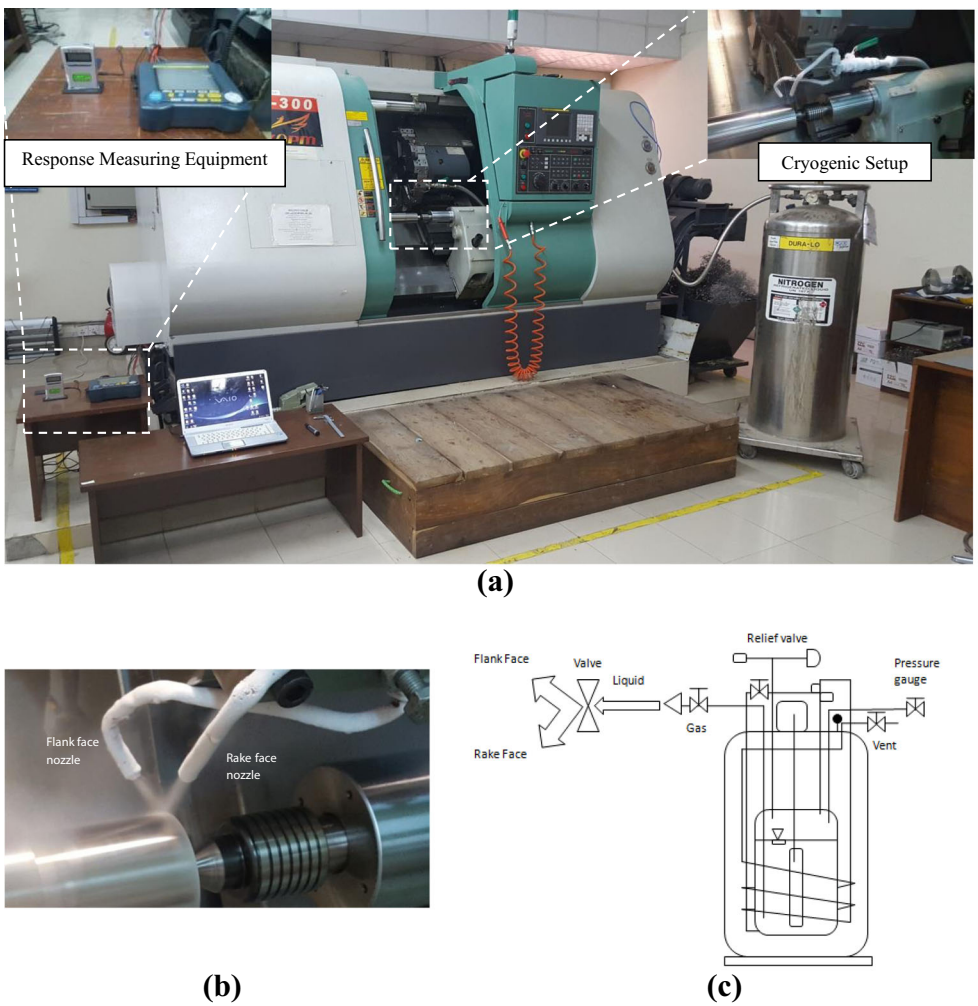

Fig. 2 Cryogenic experimental setup (**a**) CNC turning center with response measuring equipment and cryogenic setup (**b**) dual nozzle configuration (**c**) cryogenic cylinder schematic diagram

$$\mathrm{MRR} = \mathrm{f} \times \mathrm{V} \times \mathrm{d} \tag{5}$$

3.5 Design of experiment

Taguchi design of experiments (devised by Genichi Taguchi [48]) was used to formulate an orthogonal L9 array. Taguchi method was preferred due to its efficiency in having lesser numbers of runs required [49, 50]. Taguchi orthogonal arrays which are utilized as per the factors and their levels are known to produce conclusive results [51]. Various past researchers have used it effectively [26, 36, 52, 53]. Experimental runs were repeated to measure responses twice. Average values of measured responses are displayed against their machining parameters combinations in Table 4.

Table 3 Cutting parameters with levels

Parameter	Level 1	Level 2	Level 3
Feed (mm/rev)	0.12	0.16	0.20
Cutting speed (m/min)	50	100	150
Depth of cut (mm)	1	1.5	2
Cutting condition (CC)	Dry	Wet	Cryogenic

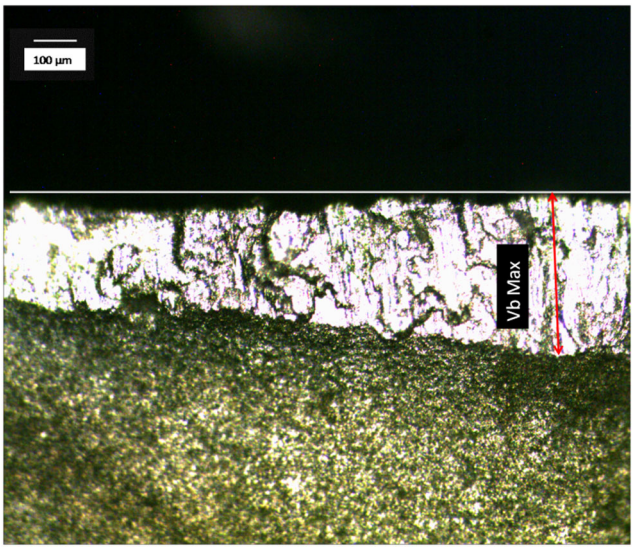

Fig. 3 Flank wear analysis using optical microscope imagery

4 Analysis

Effects of various input cutting parameters are plotted as shown in Fig. 4. All four responses are plotted on the same plane, separately for each input. It gives a comparative view of output responses as the input varies throughout its domain. Each input was analyzed individually.

4.1 Effect of feed

Feed (axial travel of tool) is a significant machining parameter having profound effects on responses as evident from Fig. 4(a). R, Ra, and MRR are increasing with increasing feed whereas SCE decreases. In contribution to the low thermal conductivity of titanium alloy, R increases with increasing feed as the heat dissipation rate recedes [54]. Diffusion dissolution and abrasion wear which are the primary causes of tool wear increases manifold with increasing temperature resulting in high R [41]. Feed influences Ra mainly because of its geometric contribution. Higher Ra with increasing feed is due to the higher peaks and crest on the machined surface [55]. Also, the increased vibration at tool-workpiece interface at higher feed values adds to Ra [56]. Besides the localized heat in titanium which induces thermal softening and lowers SCE, the elevated shear angle at higher feed values reduces SCE [57]. MRR relation with feed is linear as shown by Eq. 2.

4.2 Effect of speed

Speed as an input parameter is taken in linear terms for example in this study from 50 m/min to 150 m/min. However, it is fed after conversion into radial speed (RPM). Schulz and Moriwaki [58] has categorized different machining ranges for different materials based on speed as shown in Fig. 5. Here, titanium transitional machining ranges from 60 to 120 m/min. In the present research findings, increasing speed increases R, SCE, and MRR, whereas Ra decreases during this transition as shown in Fig. 4(b). Cutting zone temperature increases sharply with increase in cutting speed [59]. Titanium alloy cutting zone temperature can reach around 800 °C [60] which significantly accelerates wear [41]. On the other hand, increasing the cutting speed reduces Ra as chatter, which is induced by the built-up edge (BUE) at low speed, diminishes [61]. The phenomena of work hardening of titanium alloys at high cutting speeds increases the specific cutting energy by increasing the bearing loads [36, 62]. Also, the aggravated tool wear because of the high temperature strength of titanium alloys and material adhesion on cutting edge contributes to specific cutting energy [43]. It is reported [63, 64] that the phenomenon of decreasing cutting forces with increasing temperature is a material-based property and mainly depends on the speed range under consideration. MRR has increased with speed because of its direct relationship as already highlighted.

4.3 Effect of depth of cut

Depth of cut is a relatively less effective parameter as compared to feed and speed. Although it is inconsistent with R and Ra, MRR is directly dependent on it. Increasing depth of cut increases MRR as the amount of removed material increases. Power consumption is directly proportional to the material removed. Even with increased power consumption, SCE decreases because MRR increases at a higher rate than power. This is evident from the main effects plot as shown in Fig. 4(c).

4.4 Effect of machining environment

Dry, wet, and cryogenic cutting conditions were used in this research which differs not only in their cooling capacity but also their lubrication effect. Dry condition has no extra mechanism for heat extraction which results in highest R followed by wet condition [65]. Cryogenic cooling which has an extremely lower temperature (− 197 °C [18]) significantly reduces R as wear mechanism mainly depends on cutting zone temperature [66]. Reduction of cutting zone temperature by use of cryogenic media is mainly because of prevention of heat generation and to a lesser extent by swift heat extrication [18]. Ra improves under wet and cryogenic conditions due to the added lubrication effect of coolant [17]. Cryogenic results are better because of the coolant plus lubricant effect. Lubrication gains are less pronounced at higher speed due to the difficulty of penetration of media into the cutting zone [67]. It is also reported that tool-work tribology significantly alters due to coolant usage in terms of reduction in coefficient of friction [68].

SCE is lower under dry conditions than wet because of the thermal softening gain at higher temperatures. However, the work hardening of titanium alloys which is the main reason of increasing SCE lowers with temperature [69]. This causes cryogenic to reduce energy consumption owing to its extremely low temperature. Results are in line with the findings reported by earlier researchers [19, 35, 36, 47].

4.5 Optimization of individual process responses

In this study R, Ra, and SCE were based on smaller is better model whereas MRR was based on larger is better. Table 5 displays the desired values of input parameters for optimizing selective responses individually as deduced from the main effects plot presented earlier. Figure 6 shows the flank wear of tools used in best and worst experiments in terms of wear.

Table 4 Taguchi array along with the measured responses

Run	f (mm/rev)	V (m/min)	d (mm)	Cutting Conditions*	Wear rate R	Ra (μm)	SCE (J/mm^3)	MRR (cm^3/s)
1	0.12	50	1	1	− 6.1864	1.52	1.1254	0.0999
2	0.12	100	1.5	2	− 6.1603	1.20	1.2671	0.2998
3	0.12	150	2	3	− 5.9464	1.14	1.2171	0.5997
4	0.16	50	1.5	3	− 6.2015	1.83	1.0409	0.1999
5	0.16	100	2	1	− 5.7817	1.76	1.1911	0.5331
6	0.16	150	1	2	− 5.7683	1.62	1.3380	0.3998
7	0.20	50	2	2	− 5.9425	2.97	1.0954	0.3332
8	0.20	100	1	3	− 5.8803	2.62	1.1404	0.3332
9	0.20	150	1.5	1	− 5.1824	2.67	1.2605	0.7497

*1 = dry, 2 = wet, and 3 = cryogenic

4.6 Need for multi-objective optimization

Analysis of Table 5 highlights that different responses optimize at different values of input variables. This differing situation brought up the need to draw a balance between all the responses through MOO.

5 Multi-objective optimization using gray relational analysis

MOO is the way forward towards the research goal of achieving optimum multiple responses simultaneously. Technique used in this research was introduced by Deng Julong [70] in 1989. The concept of gray system was first floated by Deng Julong in 1981 [71] in which it was explained as something which is not explicit in black or white, hence gray. The idea was to process the available data in a way to make decision-making possible. Gray relational grade was first proposed in 1985 by Wang Ting [72] . The process consists of a few steps [27, 28, 31, 36] which will be explained briefly one by one. Methodology used in this research is shown in Fig. 7.

5.1 Pre-processing measured data

In this step, each response value was brought to a common scale with extremes at 0 and 1. R, Ra, and SCE are normalized using Eq. (6) as they are based on smaller the better model whereas MRR is normalized using Eq. (7) being based on larger the better model.

$$Z_{ij} = \frac{\max\left(y_{ij}, i = 1, 2, \ldots..n\right) - y_{ij}}{\max\left(y_{ij}, i = 1, 2, \ldots..n\right) - \min\left(y_{ij}, i = 1, 2, \ldots..n\right)} \tag{6}$$

$$Z_{ij} = \frac{y_{ij} - \min\left(y_{ij}, i = 1, 2, \ldots..n\right)}{\max\left(y_{ij}, i = 1, 2, \ldots..n\right) - \min\left(y_{ij}, i = 1, 2, \ldots..n\right)} \tag{7}$$

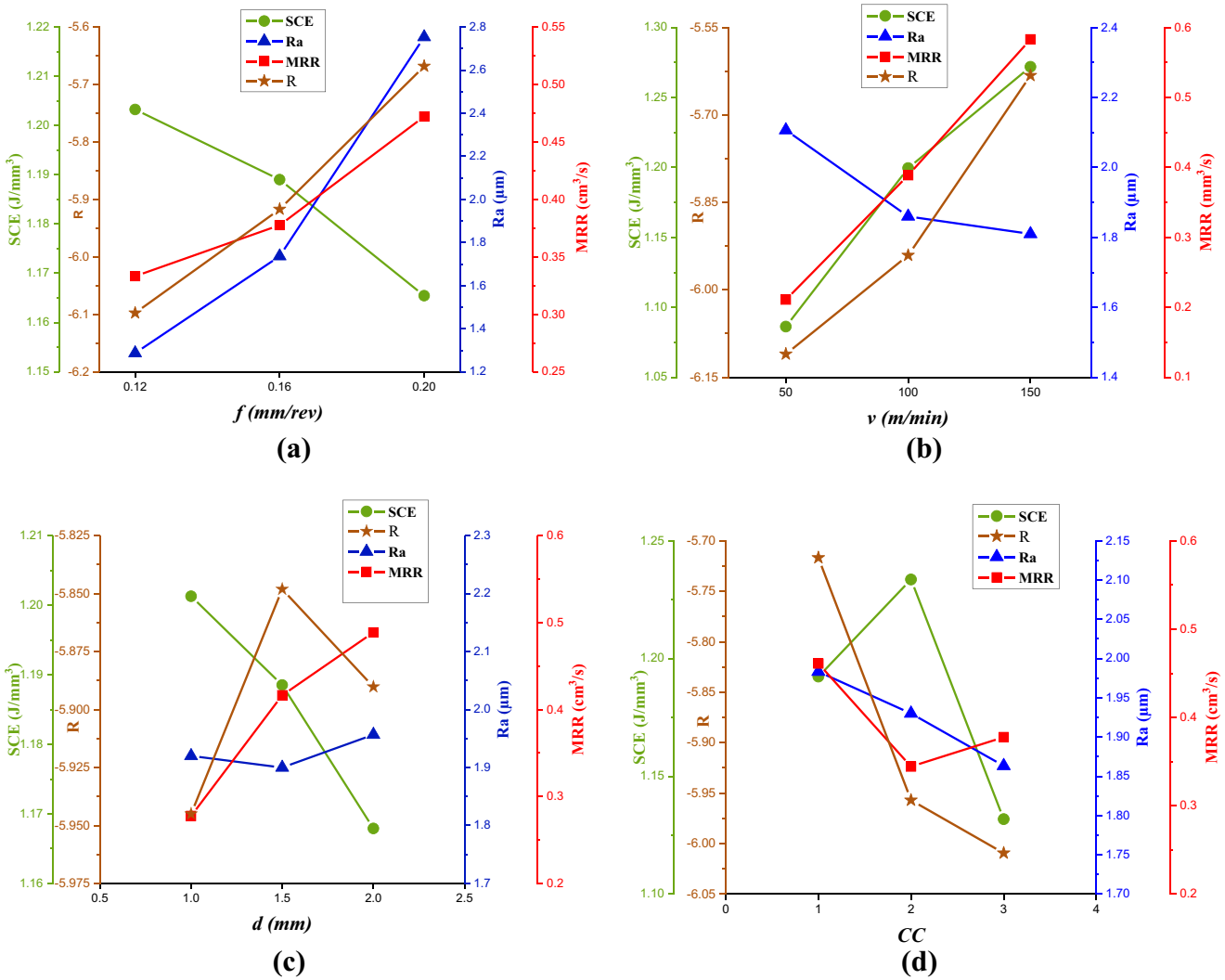

Fig. 4 Effect of machining parameters on responses (**a**) effect of feed (**b**) effect of speed (**c**) effect of depth of cut (**d**) effect of machining environment

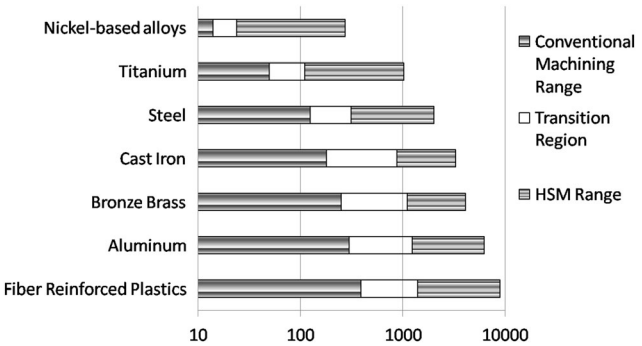

Fig. 5 Cutting speed categories for machining of different materials [58]

Here j = 1, 2, …m and I = 1, 2, …*n* where m is the number of responses studied and index *n* is the count of experimental data parameters.

5.2 Gray relational coefficient (GRC) calculation

After data processing, Eq. (8) is used to calculate gray relational coefficient [73].

$$\gamma\left(Z_o, Z_{ij}\right) = \frac{\Delta\min + \xi\Delta\max}{\Delta_{oj}(k) + \xi\Delta\max} \tag{8}$$

Here, value of $\gamma\ (Z_o, Z_{ij})$ is greater than 0 and less than or equal to 1.$Z_{ij}(k)$ and $Z_o(k)$ are the comparability and reference sequences, respectively, where $Z_o(k) = 1$, k= 1…m. Also, deviation sequence is computed from Eq. (9).

$$\Delta_{oj}(k) = |\ Z_o(k) - Z_{ij}(k)| \tag{9}$$

Δmin and Δmax corresponds to the smallest and largest values of $\Delta_{oj}(k)$. ξ, is known as the distinguishing coefficient which is kept equal to 05 if all parameters have same weightage. Generally $\xi, \epsilon\ |0, 1|$

5.3 Gray relational grade (GRG) calculation

In this step, the varying multiple objectives are converted into single gray relational grade (GRG). Optimum results can be produced by maximizing the obtained GRG. Eq. (10) is used to compute GRG where ω_r is the weight of r^{th} objective.

Table 5 Machining parameter combinations for individual best and worst responses

Input parameters	Responses							
	Wear rate, R		SCE (J/mm^3)		Ra (μm)		MRR (cm^3/s)	
	Best	Worst	Best	Worst	Best	Worst	Best	Worst
f (mm/rev)	0.12	0.20	0.20	0.12	0.12	0.20	0.20	0.12
v (m/min)	50	150	50	150	150	50	150	50
d (mm)	1	1.5	2	1	1.5	2	2	1
CC	3	1	3	2	3	1	–	–

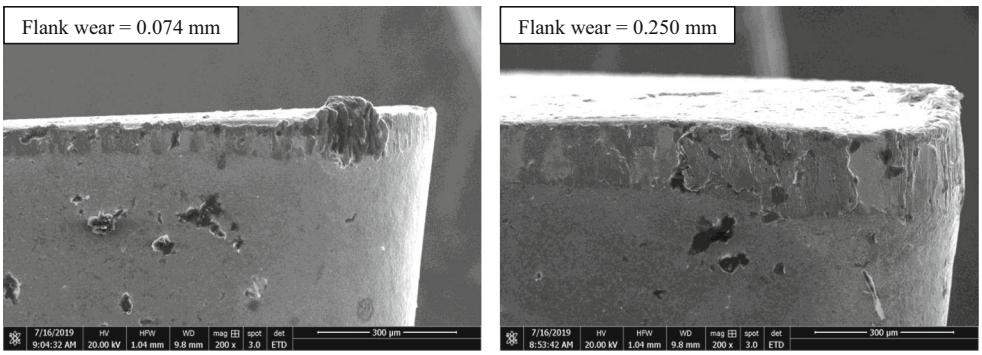

Fig. 6 Scanning electron microscopy images (**a**) Min wear at 0.16,50,1.5,cryogenic (**b**) max wear at 0.2,150,1.5,dry

Weight is determined by manufacturer through customer re-quirement or prescribed policy. In the present research, all responses are given equal weight [31, 35].

$$\text{Grade}\left(Z_o, Z_{ij}\right) = \sum_{r=1}^{n} \omega_r\, \gamma\left(Z_o, Z_{ij}\right) \tag{10}$$

$$\sum_{r=1}^{n} \omega_r = 1 \tag{11}$$

5.4 GRG order

All the experimental runs were then ranked from 1 to 9 with respect to their corresponding GRG values. Optimum run is identified with highest GRG value and is ranked number 1. This condition indicates the ideal machining parameters for concurrent optimization of the machining process. GRG ranking of the experimental runs is shown in Table 6. Experiment# 4 displayed the highest value of GRG with input parameters of feed 0.16 mm/rev, speed 50 m/min, and depth of cut 1.5 mm under cryogenic condition.

6 Regression analysis

An elaborate regression analysis was carried out including regression modeling and its optimization. Analysis of variance was used to identify significant contributing parameters followed by validation experiments. Step-wise analysis is as follows.

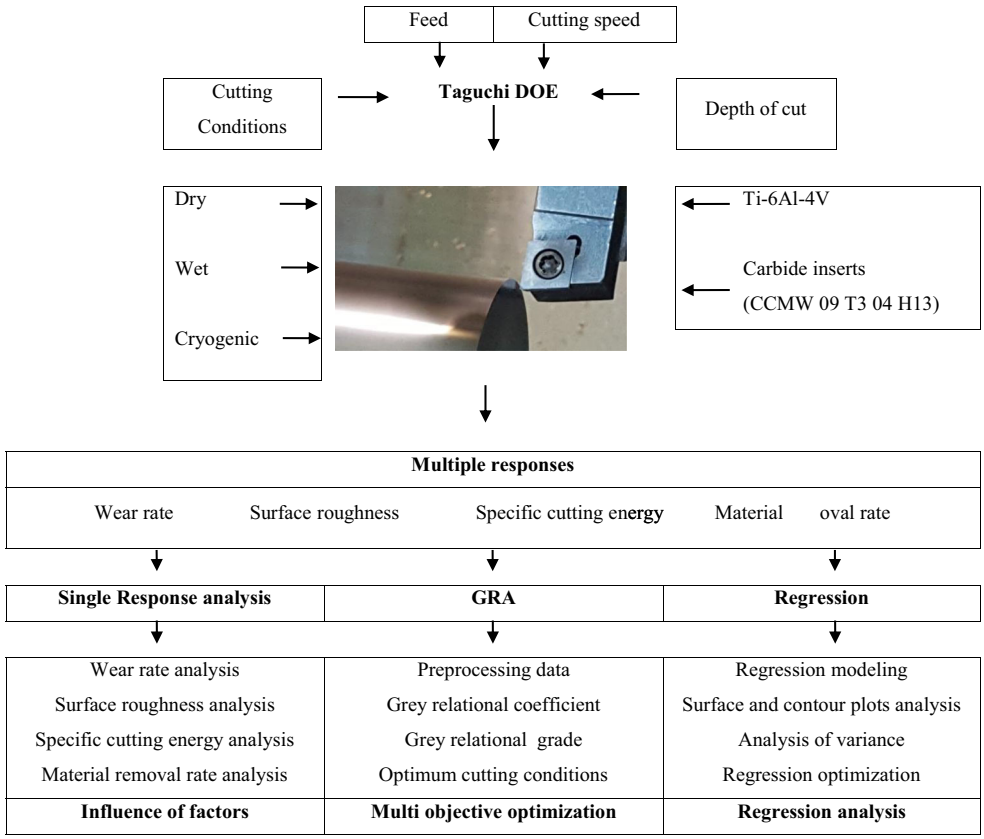

Fig. 7 Methodology for multi-objective optimization used in this research

6.1 Regression modeling of multi-objective function

Regression modeling was carried out and optimized using RSM. In the present research, machining environment was a noncontinuous categorical factor having three distinct levels, i.e., dry, wet, and cryogenic. A separate function for each cutting condition was formulated as shown at Eq. 11, Eq. 12, and Eq. 13, respectively.

$$GRG\,(f, V, d, dry) = 0.166 - 0.42f - 0.00247V + 0.945d - 3.97f*f + 0.000010V*V - 0.2947\,d*d \quad (11)$$

$$GRG\,(f, V, d, wet) = 0.171 - 0.42f - 0.00247V + 0.945d - 3.97f*f + 0.000010V*V - 0.2947\,d*d \quad (12)$$

$$GRG\,(f, V, d, cryogenic) = 0.248 - 0.42f - 0.00247V + 0.945d - 3.97f*f + 0.000010V*V - 0.2947\,d*d \quad (13)$$

Table 6 GRC values for R, Ra, SCE, and MRR; and GRG for each experiment

Exp	f (mm/rev)	V (m/min)	d (mm)	Cutting conditions (CC)	Gray relational coefficients				GRG	Rank
					GRC (R)	GRC (Ra)	GRC (SCE)	GRC (MRR)		
1	0.12	50	1	1	0.9712	0.7066	0.6317	0.3333	0.6607	4
2	0.12	100	1.5	2	0.9251	0.9385	0.3956	0.4194	0.6696	3
3	0.12	150	2	3	0.6664	1.0000	0.4557	0.6842	0.7016	2
4	0.16	50	1.5	3	1.0000	0.5701	1.0000	0.3714	0.7354	1
5	0.16	100	2	1	0.5483	0.5961	0.4948	0.6000	0.5598	5
6	0.16	150	1	2	0.5405	0.6559	0.3333	0.4815	0.5028	9
7	0.20	50	2	2	0.6630	0.3333	0.7228	0.4382	0.5393	6
8	0.20	100	1	3	0.6134	0.3820	0.5941	0.4382	0.5069	8
9	0.20	150	1.5	1	0.3333	0.3742	0.4027	1.0000	0.5276	7

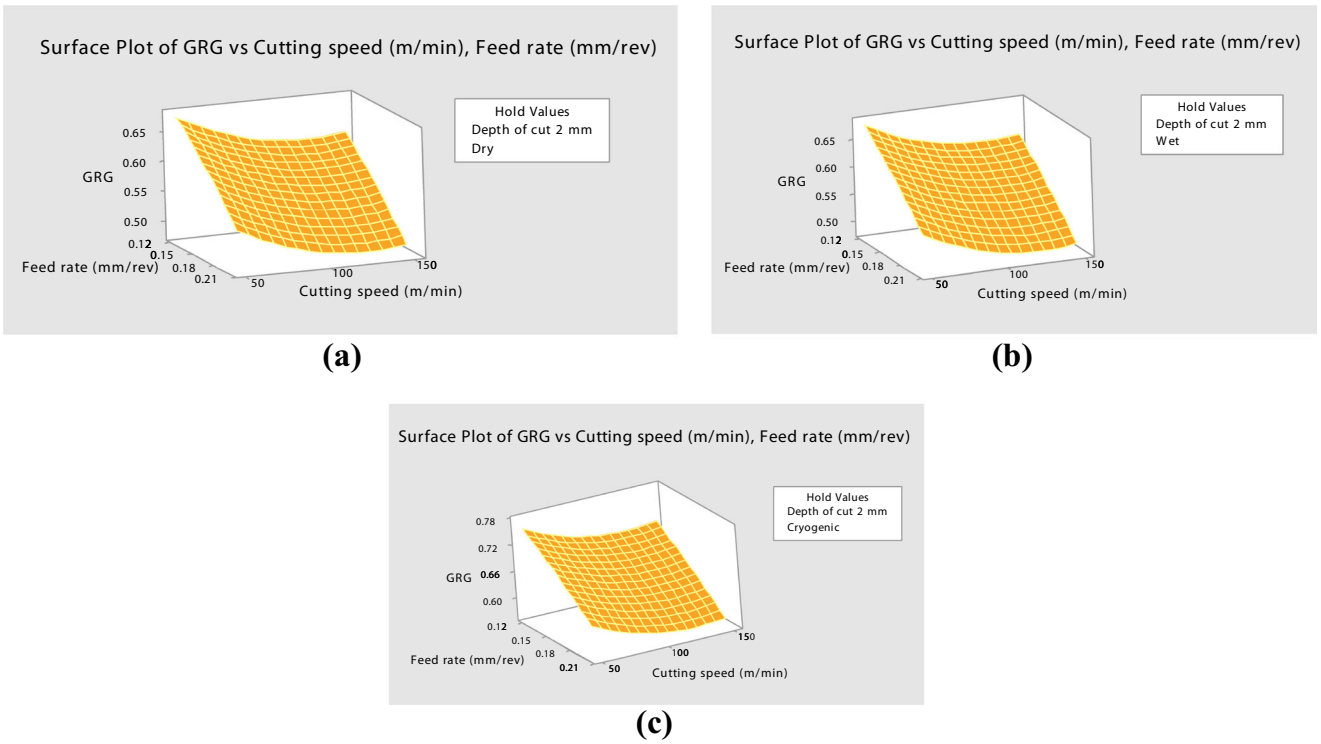

Fig. 8 Surface plots of GRG vs machining parameters (**a**) dry (**b**) wet (**c**) cryogenic conditions

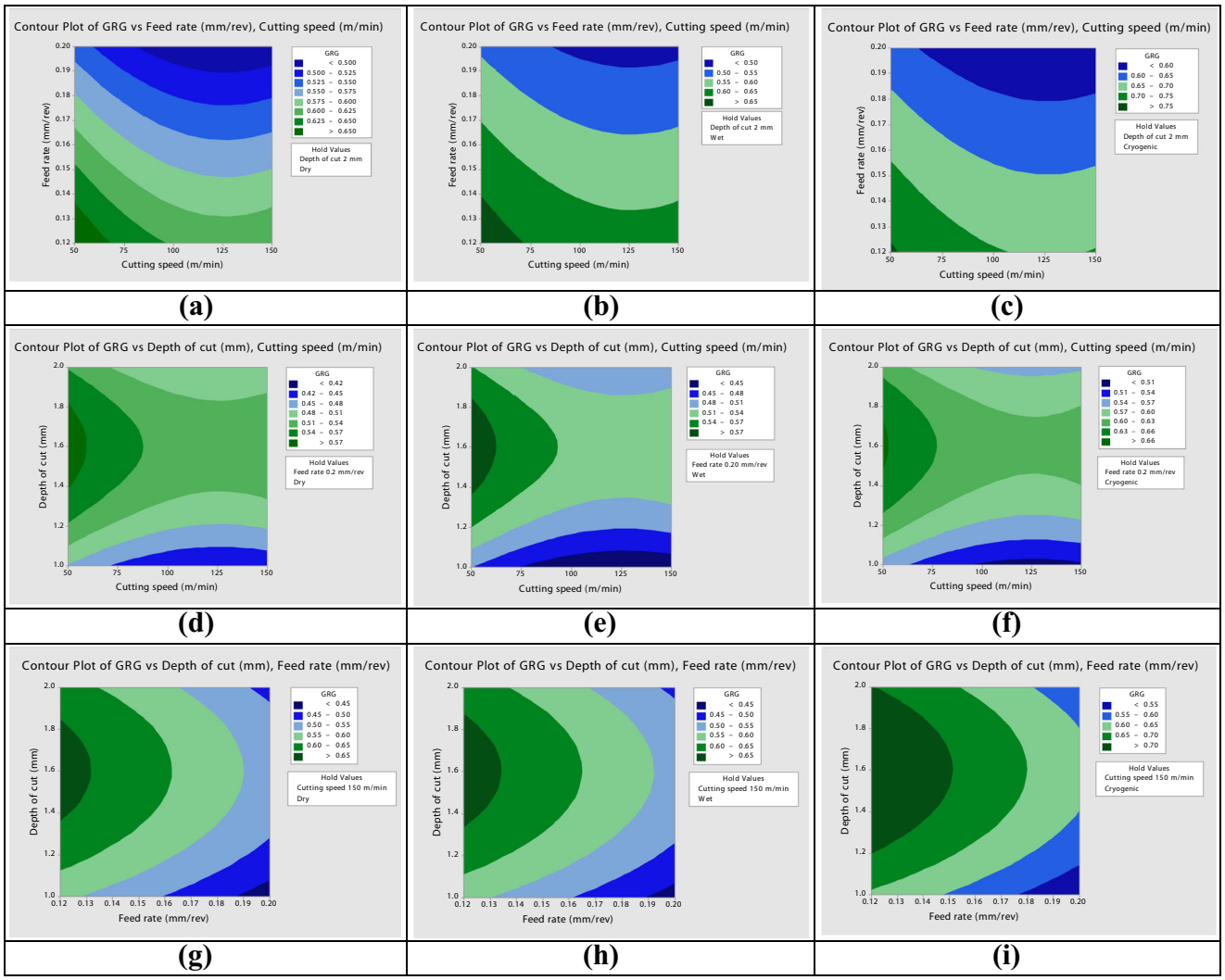

Fig. 9 Contour plots of GRG vs machining parameters (**a**) speed vs feed, dry (**b**) speed vs feed, wet (**c**) speed vs feed, cryogenic (**d**) speed vs depth of cut, dry (**e**) speed vs depth of cut, wet (**f**) speed vs depth of cut,cryogenic (g) feed vs depth of cut, dry (h) feed vs depth of cut, wet (i) feed vs depth of cut, cryogenic

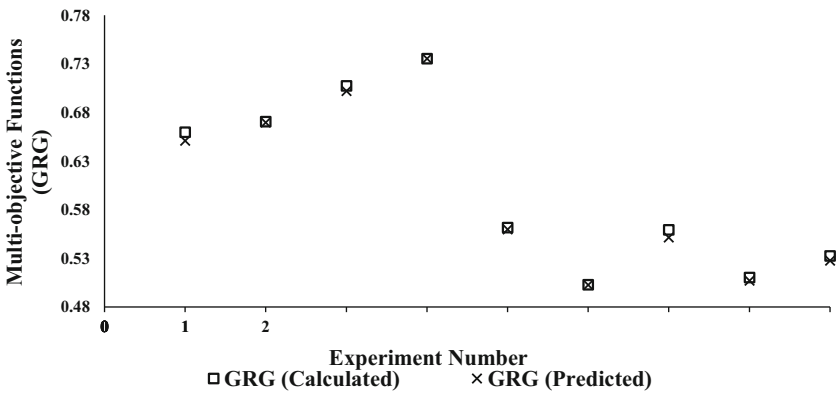

Fig. 10 Comparison of GRG calculated from regression model and obtained experimentally

The main difference between the above three equations is the positive intercept value. Cryogenic condition has a positive intercept gain of 45% and 51% on wet and dry conditions, respectively. Above three equations hold good for all values of input parameters. Figure 8 displays the surface plots of GRG at different machining parameters for dry, wet, and cryogenic conditions. It can be seen that higher values of GRG is measured towards lesser values of feed and speed, with cryogenic GRG being highest of the three conditions. Fig. 9 displays the contour plots of GRG at different machining parameters for dry, wet, and cryogenic conditions. The two tone results of dry and wet are comparable as there is slight difference with wet machining having an edge over dry machining. However, clear shift towards the higher side can be seen in plots of cryogenic machining. In other words, for same machining parameters, cryogenic conditions give an overall advantage over dry and wet machining. A comparison between the values of GRG determined from model and obtained experimentally is shown in Fig. 10. Maximum deviation of 2% is obtained which indicates substantial validity of model.

6.2 Analysis of variance (ANOVA)

Table 7 displays the ANOVA of regression model. Contribution ratio of feed was found highest at 42.36% whereas cutting condition stood second with contribution ratio of 19.63%. Depth of cut and cutting speed showed contributions of 8.69% and 6.14%, respectively. Among square terms depth of cut proved significant with 16.79% contribution.

6.3 Regression model optimization

Response surface optimization was used to find the correct combination of machining parameters for optimum output response. Result is shown in Fig. 11. Further they were experimentally validated.

6.4 Validation experiments

Machining parameters optimized through RSM along with best run condition in initial experiments (experiment # 4) are tabulated in Table 8. Validation of these conditions was carried out with results showing significant improvement. R and Ra improved by 30% and 22%, respectively, whereas SCE improved by 4%.

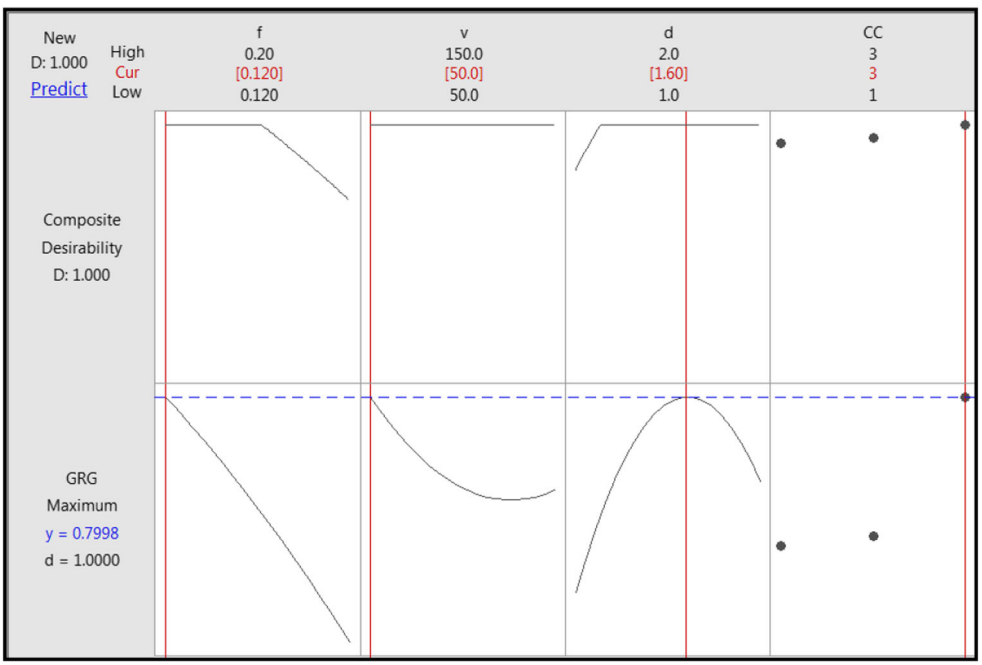

Fig. 11 Response surface optimization of GRG

Table 7 Analysis of variance for regression model

Source	DF	Seq SS	Adj MS	Seq MS	F	P	CR
Regression model	8	0.123614	0.123614	0.015452	24.29	0.000	95.57%
Linear	5	0.099356	0.099356	0.019871	31.23	0.000	76.82%
f (mm/rev)	1	0.054792	0.000017	0.054792	86.12	0.000	42.36%
V (m/min)	1	0.007941	0.003721	0.007941	12.48	0.006	6.14%
d (mm)	1	0.011236	0.024601	0.011236	17.66	0.002	8.69%
Cutting conditions (CC)	2	0.025386	0.025386	0.012693	19.95	0.000	19.63%
Square	3	0.024258	0.024258	0.008086	12.71	0.001	18.76%
f*f	1	0.000162	0.000162	0.000162	0.25	0.626	0.12%
V*V	1	0.002378	0.002378	0.002378	3.74	0.085	1.84%
d*d	1	0.021718	0.021718	0.021718	34.13	0.000	16.79%
Error	9	0.005726	0.005726	0.000636			4.43%
Total	17	0.129340					100%

S = 0.0252242 R-Sq = 94.64% R-Sq.(pred) = 85.29%

DF, degrees of freedom; SS, sum of squares; MS, mean squares; F, F value; P, *P* value; CR, contribution ratio (%); S, standard deviation; R-Sq.(pred) predicted R^2

Table 8 Comparison of optimized run with best initial experimental run # 4

	Machining conditions				Responses			
	f	V	d	CC	R	Ra	SCE	MRR
Best run	0.16	50	1.5	3 (Cryo)	− 6.2015	1.83	1.0409	0.1999
Optimized run	0.12	50	1.6	3 (Cryo)	− 6.3502	1.44	1.0004	0.1609

7 Conclusion

Present research focused on sustainability, productivity, and efficiency of machining process by turning Ti-6Al-4 V under dry, wet, and cryogenic conditions. SCE, R, Ra, and MRR were chosen as the performance output parameters where the first two represents sustainability and efficiency and last two advocates for productivity of machining processes. Based on this work the following conclusions can be chalked:

- Cryogenic coolant being applied in dual nozzle configuration has played an effective role in reducing R, Ra, and SCE. Out of all the initial experiments run, # 4 was found to give the collective optimum results. R and Ra were further reduced by 30% and 22%, respectively, whereas SCE was improved by 4% when cryogenic machining was carried out at optimum conditions.
- Wet machining showed better results in terms of R and Ra than dry machining. Nevertheless, the thermal softening at higher temperatures resulted in lower SCE consumption for dry machining.
- ANOVA results identified feed as the most influential parameter with 42.36% contribution ratio followed by cutting conditions (19.63%). While among interaction parameters, d*d was significant with 16.79% contribution ratio.
- Regression analysis showed GRG gain for cryogenic environment over wet and dry conditions as 45% and 51%, respectively. This highlights the benefits of using cryogenic media in collectively improving the machining process.
- Specific cutting energy is a material-based property as it depends on a number of external and inherent factors. Work hardening of titanium alloys which increases SCE at elevated speeds tends to lower with temperature especially with cryogenic temperatures.
- Surface roughness improves under wet and cryogenic machining environment due to their added lubrication effect.

It is imperative to highlight the benefit of using a suitable coolant at an already optimized machining condition. It can significantly contribute towards sustainability, productivity, and efficiency of machining process by increasing productivity and reducing cost. The effects of cryogenic as an input variable in subsurface characterization and chip morphology needs investigation and will be taken up in future. In addition, wear progression under cryogenic media merits research in order to quantitatively compare the benefits of cryogenic. This will serve in moving towards the prime objective of sustainable manufacturing.

References

1. Yi S, Jang Y-C, An AK (2018) Potential for energy recovery and greenhouse gas reduction through waste-to-energy technologies. J Clean Prod 176:503–511
2. Zhou L, Li J, Li F, Meng Q, Li J, Xu X (2016) Energy consumption model and energy efficiency of machine tools: a comprehensive literature review. J Clean Prod 112:3721–3734
3. Kara S, Li W (2011) Unit process energy consumption models for material removal processes. CIRP Ann 60:37–40
4. Birol F (2017) Key world energy statistics. International Energy Agency, Paris
5. Zhao G, Hou C, Qiao J, Cheng X (2016) Energy consumption characteristics evaluation method in turning. Adv Mech Eng 8:1–8
6. Tonshoff H, Wobker H, Brandt D (1996) Tool wear and surface integrity in hard turning. Prod Eng 3:19–24
7. Hughes J, Sharman A, Ridgway K (2006) "the effect of cutting tool material and edge geometry on tool life and workpiece surface integrity," Proceedings of the Institution of Mechanical Engineers. Part B: J Eng Manuf 220:93–107
8. López de lacalle LN, Pérez J, Llorente JI, Sánchez JA (2000) Advanced cutting conditions for the milling of aeronautical alloys. J Mater Process Technol 100:1–11
9. Barry J, Byrne G, Lennon D (2001) Observations on chip formation and acoustic emission in machining Ti–6Al–4V alloy. Int J Mach Tools Manuf 41:1055–1070
10. Hong SY, Markus I, Jeong W-c (2001) New cooling approach and tool life improvement in cryogenic machining of titanium alloy Ti-6Al-4V. Int J Mach Tools Manuf 41:2245–2260
11. Sivaiah P, Chakradhar D (2018) Effect of cryogenic coolant on turning performance characteristics during machining of 17-4 PH stainless steel: a comparison with MQL, wet, dry machining. CIRP J Manuf Sci Technol 21:86–96
12. Sun Y, Huang B, Puleo DA, Jawahir IS (2015) Enhanced machinability of Ti-5553 alloy from cryogenic machining: comparison with MQL and flood-cooled machining and modeling. Procedia CIRP 31:477–482
13. Kaynak Y, Lu T, Jawahir IS (2014) Cryogenic machining-induced surface integrity: a review and comparison with dry, MQL, and flood-cooled machining. Mach Sci Technol 18:149–198
14. Senevirathne SWMAI, Punchihewa HKG (2017) Comparison of tool life and surface roughness with MQL, flood cooling, and dry cutting conditions with P20 and D2 steel. IOP Conference Series: Materials Science and Engineering 244:012006
15. Khatri A, Jahan MP (2018) Investigating tool wear mechanisms in machining of Ti-6Al-4V in flood coolant, dry and MQL conditions. Procedia Manufacturing 26:434–445
16. Aramcharoen A (2016) Influence of cryogenic cooling on tool wear and chip formation in turning of titanium alloy. Procedia CIRP 46: 83–86
17. Bagherzadeh A, Budak E (2018) Investigation of machinability in turning of difficult-to-cut materials using a new cryogenic cooling approach. Tribol Int 119:510–520
18. Bermingham MJ, Kirsch J, Sun S, Palanisamy S, Dargusch MS (2011) New observations on tool life, cutting forces and chip morphology in cryogenic machining Ti-6Al-4V. Int J Mach Tools Manuf 51:500–511
19. Bordin A, Bruschi S, Ghiotti A, Bariani PF (2015) Analysis of tool wear in cryogenic machining of additive manufactured Ti6Al4V alloy. Wear 328-329:89–99
20. Hong SY, Ding Y, Ekkens RG (1999) Improving low carbon steel chip breakability by cryogenic chip cooling. Int J Mach Tools Manuf 39:1065–1085
21. Lu T, Kudaravalli R, Georgiou G (2018) Cryogenic machining through the spindle and tool for improved machining process performance and sustainability: Pt. I, system design. Procedia Manuf 21:266–272
22. Zhao Z, Hong S (1992) Cooling strategies for cryogenic machining from a materials viewpoint. J Mater Eng Perform 1:669–678
23. Shokrani A, Dhokia V, Newman ST (2012) Environmentally conscious machining of difficult-to-machine materials with regard to cutting fluids. Int J Mach Tools Manuf 57:83–101
24. Sreejith P, Ngoi B (2000) Dry machining: machining of the future. J Mater Process Technol 101:287–291
25. Bhushan RK (2013) Optimization of cutting parameters for mini-mizing power consumption and maximizing tool life during machining of Al alloy SiC particle composites. J Clean Prod 39: 242–254
26. Camposeco-Negrete C (2015) Optimization of cutting parameters using response surface method for minimizing energy consumption and maximizing cutting quality in turning of AISI 6061 T6 aluminum. J Clean Prod 91:109–117
27. Kumar R, Bilga PS, Singh S (2017) Multi objective optimization using different methods of assigning weights to energy consumption responses, surface roughness and material removal rate during rough turning operation. J Clean Prod 164:45–57
28. Warsi SS, Agha MH, Ahmad R, Jaffery SHI, Khan M (2018) Sustainable turning using multi-objective optimization: a study of Al 6061 T6 at high cutting speeds. Int J Adv Manuf Technol 100: 843–855
29. Gupta MK, Sood PK, Singh G, Sharma VS (2017) Sustainable machining of aerospace material–Ti (grade-2) alloy: modeling and optimization. J Clean Prod 147:614–627
30. Mia M, Khan MA, Rahman SS, Dhar NR (April 01 2017) Mono-objective and multi-objective optimization of performance parameters in high pressure coolant assisted turning of Ti-6Al-4V. Int J Adv Manuf Technol 90:109–118
31. Venkata Ramana M, Rao GKM, Rao DH (2018) Multi Objective optimization of Process Parameters in Turning of Ti-6Al-4V alloy. Materials Today: Proceedings 5:18966–18974
32. Uçak N, Çiçek A (2018) The effects of cutting conditions on cutting temperature and hole quality in drilling of Inconel 718 using solid carbide drills. J Manuf Process 31:662–673
33. Sarıkaya M, Güllü A (2015) Multi-response optimization of mini-mum quantity lubrication parameters using Taguchi-based grey relational analysis in turning of difficult-to-cut alloy Haynes 25. J Clean Prod 91:347–357
34. Behera BC, Alemayehu H, Ghosh S, Rao PV (2017) A comparative study of recent lubricoolant strategies for turning of Ni-based superalloy. J Manuf Process 30:541–552
35. Mia M, Gupta MK, Lozano JA, Carou D, Pimenov DY, Królczyk G et al (2019) Multi-objective optimization and life cycle assessment of eco-friendly cryogenic N2 assisted turning of Ti-6Al-4V. J Clean Prod 210:121–133

36. Younas M, Jaffery SHI, Khan M, Ali Khan M, Ahmad R, Mubashar A et al (2019) Multi-objective optimization for sustainable turning Ti6Al4V alloy using grey relational analysis (GRA) based on analytic hierarchy process (AHP). In: The International Journal of Advanced Manufacturing Technology
37. ASTM (ed) (2015) B265–15, "Standard specification for titanium and titanium alloy strip, sheet and plate," ed. ASTM International, West Conshohocken, PA
38. Zhao Z, Hong S (1992) Cryogenic properties of some cutting tool materials. J Mater Eng Perform 1:705–714
39. Jawahir I, Attia H, Biermann D, Duflou J, Klocke F, Meyer D et al (2016) Cryogenic manufacturing processes. CIRPAnn 65:713–736
40. Hong SY (2006) Lubrication mechanisms of LN2 in ecological cryogenic machining. Mach Sci Technol 10:133–155
41. Bermingham MJ, Palanisamy S, Kent D, Dargusch MS (2012) A comparison of cryogenic and high pressure emulsion cooling technologies on tool life and chip morphology in Ti–6Al–4V cutting. J Mater Process Technol 212:752–765
42. Khan MA, Jaffery SHI, Khan M, Younas M, Butt SI, Ahmad R et al (2019) Statistical analysis of energy consumption, tool wear and surface roughness in machining of titanium alloy (Ti-6Al-4V) under dry, wet and cryogenic conditions. Mech Sci 10:561–573
43. Younas M, Jaffery SHI, Khan M, Ahmad R, Ali L, Khan Z et al (2019) Tool Wear progression and its effect on energy consumption in turning of titanium alloy (Ti-6Al-4V). Mech Sci 10:373–382
44. ISO Standard (1993) "ISO-3685," Tool-life Testing with Single Point Turning Tools
45. Sandvik (2015) Sandvik launches CBN tool for hard-part turning. Metal Powder Report 70:312–313
46. Li W, Kara S (2011) "An empirical model for predicting energy consumption of manufacturing processes: a case of turning process," *Proceedings of the Institution of Mechanical Engineers*. Part B: J Eng Manuf 225:1636–1646
47. Warsi SS, Jaffery SHI, Ahmad R, Khan M, Ali L, Agha MH et al (2017) "development of energy consumption map for orthogonal machining of Al 6061-T6 alloy," *Proceedings of the Institution of Mechanical Engineers*. Part B: J Eng Manuf 232:2510–2522
48. Taguchi G, Yokoyama Y (1993) Taguchi methods: design of experiments. Amer Supplier Inst 4
49. Ross PJ, Ross PJ (1988) Taguchi techniques for quality engineering: loss function, orthogonal experiments, parameter and tolerance design. McGrawhill, New York
50. Ziegel ER (1997) Taguchi techniques for quality engineering. Taylor & Francis Group
51. Black J, Kohser R (2008) Materials & Processes in Manufacturing. John Wiley&Sons," ed: Inc
52. Ravi Kumar SM, Kulkarni SK (2017) Analysis of hard machining of titanium alloy by Taguchi method. Materials Today: Proceedings 4:10729–10738
53. Davis R, Singh V, Priyanka S (2014) Optimization of process parameters of turning operation of EN 24 steel using Taguchi Design of Experiment Method. In: Proceedings of the World Congress on Engineering
54. Sarwar M, Persson M, Hellbergh H, Haider J (2009) Measurement of specific cutting energy for evaluating the efficiency of bandsawing different workpiece materials. Int J Mach Tools Manuf 49:958–965
55. Mia M, Dhar NR (2016) Prediction of surface roughness in hard turning under high pressure coolant using artificial neural network. Measurement 92:464–474
56. Yan J, Li L (2013) Multi-objective optimization of milling parameters–the trade-offs between energy, production rate and cutting quality. J Clean Prod 52:462–471
57. Groover MP (2007) Fundamentals of modern manufacturing: materials processes, and systems. John Wiley & Sons, New York
58. Schulz H, Moriwaki T (1992) High-speed machining. CIRP Ann 41:637–643
59. Fan Y, Hao Z, Zheng M, Yang S (2016) Wear characteristics of cemented carbide tool in dry-machining Ti-6Al-4V. Mach Sci Technol 20:249–261
60. Shaw MC (2005) Metal cutting principles. Oxford university press, New York
61. Mia M, Dhar NR (2017) Optimization of surface roughness and cutting temperature in high-pressure coolant-assisted hard turning using Taguchi method. Int J Adv Manuf Technol 88:739–753
62. Jaffery SI, Mativenga PT (2008) Assessment of the machinability of Ti-6Al-4V alloy using the wear map approach. Int J Adv Manuf Technol 40:687–696
63. Schulz H, Arnold W, Scherer J (1981) High speed machining: new technology or slogan? Werkstatt und Betrieb 114:527–531
64. Komanduri R, Subramanian K, von Turkovich B (1984) High speed machining: presented at the winter annual meeting of the American Society of Mechanical Engineers. New Orleans, Louisiana
65. Ali Khan M, Husain Imran S (2019) Jaffery, M. Khan, and S. Ikramullah butt, "Wear and surface roughness analysis of machining of Ti-6Al-4V under dry, wet and cryogenic conditions," *IOP Conference Series*. Mater Sci Eng 689:012006
66. Dhar N, Kamruzzaman M (2007) Cutting temperature, tool wear, surface roughness and dimensional deviation in turning AISI-4037 steel under cryogenic condition. Int J Mach Tools Manuf 47:754–759
67. Venugopal KA, Paul S, Chattopadhyay AB (2007) Growth of tool wear in turning of Ti-6Al-4V alloy under cryogenic cooling. Wear 262:1071–1078
68. Strano M, Chiappini E, Tirelli S, Albertelli P, Monno M (2013) "comparison of Ti6Al4V machining forces and tool life for cryogenic versus conventional cooling," *Proceedings of the Institution of Mechanical Engineers*. Part B: J Eng Manuf 227:1403–1408
69. Chichili D, Ramesh K, Hemker K (1998) The high-strain-rate response of alpha-titanium: experiments, deformation mechanisms and modeling. Acta Mater 46:1025–1043
70. Julong D (1989) Introduction to grey system theory. The Journal of grey system 1:1–24
71. Julong D (1982) Control problems of grey systems. Sys & Contr Lett 1:288–294
72. Wang T (1985) Grey functions and relational grade. Fuzzy Mathematics (Special Issue of Grey Systems) 2:59–66
73. Wojciechowski S, Maruda RW, Krolczyk GM, Niesłony P (2018) Application of signal to noise ratio and grey relational analysis to minimize forces and vibrations during precise ball end milling. Precis Eng 51:582–596